Transcription factor PROX1 suppresses Notch pathway activation via the nucleosome remodeling and deacetylase complex in colorectal cancer stem-like cells

Jenny Högström[1], Sarika Heino[1], Pauliina Kallio[1], Marianne Lähde[1], Veli-Matti Leppänen[1], Diego Balboa[2], Zoltán Wiener[1#*] and Kari Alitalo[1#]

[1] Translational Cancer Biology Research Program, University of Helsinki, FI-00014, Helsinki, Finland

[2] Molecular Neurology Program and Biomedicum Stem Cell Center, University of Helsinki, FI-00014, Helsinki, Finland

Running title: PROX1-NuRD regulation of Notch in CRC

Keywords: organoid, HDAC, LGR5, OLFM4, BirA

Equal coauthors

Disclosure of potential conflicts of interest
The authors declare no potential conflicts of interest

Correspondence: Kari Alitalo, Translational Cancer Biology Research Program, Biomedicum Helsinki, PO Box 63 (Haartmaninkatu 8), FI-00014 University of Helsinki, Finland
E-mail: kari.alitalo@helsinki.fi
Phone: +358 9 191 25511, Fax: +358 9 191 25510

*Current address: Department of Genetics, Cell- and Immunobiology, Semmelweis University, H-1089 Budapest, Hungary

Abstract

The homeobox transcription factor PROX1 is induced by high Wnt/ß-catenin activity in intestinal adenomas and colorectal cancer (CRC), where it promotes tumor progression. Here we report that in LGR5+ CRC cells, PROX1 suppresses the Notch pathway, which is essential for cell fate in intestinal stem cells. Pharmacological inhibition of Notch in *ex vivo* 3D organoid cultures from transgenic mouse intestinal adenoma models increased *Prox1* expression and the number of PROX1-positive cells. Notch inhibition led to increased proliferation of the PROX1-positive CRC cells but did not affect their ability to give rise to PROX1-negative secretory cells. Conversely, *PROX1* deletion increased Notch target gene expression and *NOTCH1* promoter activity, indicating reciprocal regulation between PROX1 and the Notch pathway in CRC. PROX1 interacted with the nucleosome remodeling and deacetylase (NuRD) complex to suppress the Notch pathway. Thus, our data suggests that PROX1 and Notch suppress each other and that PROX1-mediated suppression of Notch mediates its stem cell function in CRC.

Introduction

Activation of the Wnt pathway is the initiating event and one of the key determinants of further pathogenesis in the majority of human CRCs (1). Cellular levels of free ß-catenin are normally strictly controlled through a multiprotein complex that comprises the APC protein. Activation of the Wnt pathway prevents the proteasomal degradation of ß-catenin, which translocates to the nucleus and binds to and activates the Tcf/Lef1 transcription factors, leading to activation of target genes stimulating cell cycle progression and tumorigenesis (2). The homeobox transcription factor PROX1 is directly regulated by abnormally high levels of Wnt/ß-catenin signaling activity in CRC (3). Altered levels of PROX1 have been demonstrated in several cancers and PROX1 has been implicated in regulating cell fate in stem and progenitor cells (reviewed in 4). In the normal intestine, PROX1 is expressed in only few secretory cells

(3, 5). PROX1 expression is induced in intestinal tumor progression, where it is associated with high grade dysplasia and an invasive phenotype (3, 6). Importantly, a subpopulation of the PROX1 expressing adenoma and CRC cells displays stem cell features and deletion or silencing of *Prox1* reduces tumor size and the number of LGR5+ stem cells (3, 5).

Crosstalk between the Notch and Wnt signaling pathways has an important function in adult intestinal homeostasis (7, 8). Genetic or chemical inhibition of the Notch pathway results in reduced number of LGR5+ intestinal stem cells and accumulation of differentiated secretory cells (9, 10). In intestinal adenomas, Notch activity is regulated downstream of Wnt signaling through ß-catenin mediated transcriptional activation of the Notch ligand *Jagged1*, which contributes to intestinal tumorigenesis in $Apc^{min/+}$ mice (11). Consistently with these results, ectopic overexpression of the active NOTCH1 intracellular domain (NICD1) leads to an elevated number of adenomas in *Apc*-mutant mice (7, 12). However, despite increased numbers of tumors in $Apc^{min/+}$*;NICD1;Villin-*Cre^{ERT2} mice, these tumors were predominantly low-grade adenomas, whereas control tumors from Apc^{min} mice displayed features of high-grade adenomas, suggesting that active NOTCH1 is needed for tumor formation rather than tumor progression. Interestingly, aberrant NOTCH1 recruits the histone methyltransferase SET1 domain bifurcated 1 (SETDB1) to suppress Wnt target genes, including PROX1 (12). Although the supportive role of Notch activity in stem cells is a widely-accepted concept, these results raised the possibility that Notch activity is not required in PROX1 expressing CRC stem-like cells. Here, we set out to study the relationship between PROX1 and the Notch pathway in CRC.

Materials and Methods

In vivo experiments

The National Animal Experiment Board at the Provincial State Office of Southern Finland approved all experiments performed with mice (ESAVI/6306/04.10.07/2016 and ESAVI/7945/04.10.07/2017). All

mice were maintained in the C57Bl/6J background.

The *Apc*$^{flox/flox}$ (13), *Prox1*$^{flox/flox}$ (14) and *Lgr5-EGFP-IRES-Cre*^{ERT2} (15) mice were crossed to generate intestinal stem cell specific deletion of the *Apc* and/or *Prox1* gene. To delete *Apc* and induce tumorigenesis, 2 mg tamoxifen (Sigma #T5648) dissolved in 100 µl corn oil (Sigma #8001-30-7) was given by oral gavage at the age of 8-10 weeks. To chemically inhibit the Notch pathway, mice were given intraperitoneal injections of the γ-secretase inhibitor Dibenzazepine (DBZ) (Tocris #4489) (20 µmol/kg/day) diluted in 100 µl 0.5% (Hydroxylpropyl)methylcellulose (Sigma #H7509)-0.1% Tween20 (Acros organics #BP337-500) or vehicle on five consecutive days, starting at day 5 or day 21 after tamoxifen administration. The *in vivo* experiment was repeated twice. For each experiment, 6-10 mice were used.

To analyze the effect of Notch inhibition on Prox1 lineage tracing in intestinal adenomas, DBZ (20 µmol/kg/day) was administered intraperitoneally on four consecutive days to 16-week-old *Apc*$^{min/+}$*; Rosa26-*$^{LSL\text{-}TdTomato}$ (Jackson Laboratories, Stock 007914)*; Prox1-Cre*^{ERT2} (16) mice. Prox1 lineage tracing was activated by a single dose of 2 mg tamoxifen after the last dose of DBZ and the mice were terminated after 24 h or 72 h. The *in vivo* experiment was repeated three times. For each experiment, 10-12 mice were used.

To assess cell proliferation, mice were given one intraperitoneal injection of 1 mg/ml 5-ethynyl-2'-deoxyuridine (EdU) (Thermo Fisher Scientific #A10044) dissolved in 100 µl 0.9% NaCl and terminated four hours later. For analysis of EdU incorporation, EdU+ cells of 50-60 tumors from both groups were quantified and normalized to the total number of tumor cells.

Intestinal organoid cultures

The Ethical Committee of Helsinki University Central Hospital approved all the experiments involving patient samples. We obtained written informed consent from the patients and the studies were conducted in accordance with the Declaration of Helsinki. Tissue-biopsies from patients were processed accordingly to previously published method (17). Patient I harbored a $KRAS^{G12D}$ mutation, but neither of the patients had clinically relevant BRAF or PI3KCA mutations (6). Intestinal crypts from *Apc*$^{flox/flox}$*; villin-Cre*^{ERT2} (18), *Apc*$^{flox/flox}$*; Lgr5-EGFP-IRES-Cre*^{ERT2}, *Apc*$^{min/+}$*; Rosa26*$^{LSL-TdTomato}$*; Prox1-Cre*^{ERT2} and *Apc*$^{min/+}$*; Prox1*$^{flox/flox}$*; villin-Cre*^{ERT2} mice were isolated and cultured as previously described (5, 19). To activate gene deletion, cultures were treated with 300 nM 4-hydroxytamoxifen (4-OH-Tam) for 24 hours. Organoids with endogenously active β-catenin/TCF pathway were then selected and cultured in growth factor deficient medium. When indicated, organoids were cultured in the presence of 10 μM of DAPT (Tocris #2634) or DBZ (Tocris #4489) for five days, starting on day 3 for an early time period or day 12 for a later time period after *Apc* deletion. For determination of the replating efficiency, the organoids were extensively trypsinized to obtain clusters of 4-5 cells, which were counted and embedded into Matrigel (Corning #35623) in equal numbers. The number of organoids/well was counted under microscope 3-4 days after replating. To analyze changes in gene expression after *Apc* deletion, organoids were lysed at different time points after addition of 4-OH-Tam. Changes in gene expression were compared to normal organoids (d0).

Cell culture

The SW1222, SW620 and LS174T CRC cell lines were cultured in DMEM (Lonza #BE12-707F) + 10 % fetal bovine serum (FBS) (Biowest, S181B-500), 2 mM L-glutamine (Corning #25-005-Cl), 100 U/ml penicillin and streptomycin (Lonza #DE-17-602E). HEK293FT cells (Thermo Fisher #R70007**)** were cultured in high glucose DMEM (Gibco #11960-044) + 10% FBS, 2mM L-glutamine and 100U/ml penicillin and streptomycin. Cells were maintained at 37ºC in a humidified incubator with 5% CO_2 and

passaged every 2-4 days. The SW620 cell line was obtained from ATCC (CCL-227). The SW1222 and LS174T cell lines were a kind gift from Dr. Meenhard Herlyn, Wistar Institute (2010) and Dr. Olli Kallioniemi, Institute for Molecular Medicine Finland (2015), respectively. The SW620 and LS174T cells were originally authenticated by ATCC. All the cells were routinely authenticated by morphological inspection and expression of specific markers, and tested for mycoplasma by DAPI staining. The HEK293FT cells were used within approximately 20 passages after thawing original stocks. For experimental procedures, CRC cell lines were used between 5-15 passages after thawing. When indicated, cells were cultured in the presence of 1 μM of Entinostat (LC Laboratories #E-3866) or Vorinostat (LC Laboratories #V-8477). For analysis of "megacolony" formation (20), 1,000 SW1222 cells were embedded in Matrigel and analyzed at d10. Spheroids were imaged with EVOS FL inverted epifluorescence microscope (Thermo Fisher) using 10x or 20x LD Ph Air objectives.

Flow cytometry

Organoids were centrifuged at 1,500 rpm for 5 min and the Matrigel was removed. To obtain a single cell suspension, organoids were incubated in HBSS (Gibco #14175-053) containing 1 mg/ml collagenase type 1 (Worthington #LS004196), 1 mg/ml collagenase H (Roche #11074032001), 4 mg/ml dispase II (Sigma #04942078001) and 1000 U/ml benzonase (ChemCruz #sc-202391) for 30 min at 37°C with gentle shaking, followed by 10 min incubation with trypsin. After fixation with 2% PFA, the cells were blocked with mouse Fc block (1 μg/10^6 cells, BD biosciences #553141) and permeabilized with 1% BSA+ 0.1% Triton X-100 in HBSS. Cells were then incubated with goat anti-hPROX1 (R&D Systems #AF2727) for 20 min followed by 20 min incubation with Alexa647 donkey anti-goat secondary antibody. HBSS washes were performed in between each step. The samples were measured with a Guava EasyCyte instrument (Millipore). The flow cytometric analysis was repeated twice, using biological replicates.

Single cell RNA sequencing and data analysis

Apc$^{flox/flox}$*; villin-Cre*^{ERT2} organoids were treated with vehicle or DBZ for 5 days, starting on day 3 after *Apc* deletion. Organoids were then dissociated to obtain a single cell suspension. Cells in 0.04% BSA-PBS were analyzed using the Chromium Single-Cell 3′RNA-sequencing system (10x Genomics, Pleasanton, CA) with the Reagent Kit v2 according to the manufacturer's instructions. Briefly, the cells were loaded into Chromium Single Cell Chip v2 (10x Genomics, Pleasanton, CA) and gel beads in emulsion (GEM) generation was performed aiming at 3000 cell captures per sample. Subsequent cDNA purification, amplification (12 cycles) and library construction (sample index PCR 14 cycles) was performed as instructed. Sample libraries were sequenced on the Illumina NovaSeq 6000 system using S1 flow cell (Illumina) with following read lengths: 26bp (Read 1), 8bp (i7 Index), 0 bp (i5 Index) and 91bp (Read 2) resulting in 115 754 and 113 705 mean reads per cell for the sample vehicle and DBZ respectively. The Cell Ranger v 2.1.1 mkfastq and count pipelines (10x Genomics, Pleasanton, CA) were used to demultiplex and convert Chromium single-cell 3' RNA-sequencing barcodes and read data to FASTQ files and to generate aligned reads and gene-cell matrices. Reads were aligned to mouse reference genome mm10. We used the Seurat R package for QC, filtering and analysis of the data (21). Cells were filtered based on UMI counts and percentage of mitochondrial genes. Cells with more than 5% of mitochondrial genes were filtered out. The expression matrix was further filtered by removing genes with expression in less than 10 cells and cells with less than 800 expressed genes. The minimum expression threshold was set at 1. The final dataset consisted of 968 cells in the Vehicle sample and 1240 cells in the DBZ sample. To be able to compare the two samples, we performed canonical correlation analysis (CCA) to identify shared correlation structures and aligned the dimensions using dynamic time warping. After this we performed clustering using tSNE and set the resolution at 0.5. The single cell RNA sequencing data can be accessed from the Gene Expression Omnibus under accession number GSE118055

Plasmids

The shHDAC1 constructs (TRCN0000004817, TRCN0000004818), shHDAC2 (TRCN0000196590, TRCN0000197086), shMTA1 (TRCN0000013361, TRCN0000013362) and shScramble (SH002) were acquired from the TRC library. The *NOTCH1* promoter-based luciferase reporter was described previously (22). BirA-hPROX1 fusion protein was cloned into a FUW lentiviral vector. Myc-BirA (23) was amplified using primers GAAGCTTGGGCTGCAGGTCGACTCTAGAGCCACCATGGAACAAAAAC TCATCTCAG and AGGGCTGTGCTGTCATGGTCAGGCATAGATCCTGAGCCCTTCTCT. hPROX1 was amplified using primers ATGCCTGACCATGACAGCACAG and TTATCGATAAGCTTGATATCGAATT CGGCGCGCCCTACTCATGAAGCAGCTCTTG. Gel-purified fragments were then assembled to FUW-Xbal-Ascl-CIP. Transfection and transduction were performed as described previously (5).

BirA-mediated proximity labeling

SW1222 cells were transduced with FUW-BirA-PROX1 or FUW-BirA-NLS-Cherry lentivirus, plated at $1x10^7$ cells per sample and incubated with 50 µM biotin (Sigma Aldrich #B4501). After 24 h, the cells were washed three times with PBS, stored at −80°C and later lysed on ice for 10 min in PLCLB buffer (50 mM HEPES, 150 mM NaCl, 10% glycerol, 1% Triton X-100, 1.5 mM $MgCl_2$, 1 mM EGTA, 10 mM $Na_4P_2O_7$, 100 mM NaF), supplemented with 1.0 mM PMSF and 10 µl/ml protease inhibitor cocktail (Sigma-Aldrich #P8340), 0.1% SDS, and 80 U/ml Benzonase (ChemCruz #sc-202391), followed by three cycles of sonication and centrifugation twice at 16,000 g at 4°C to remove insoluble material. Cleared lysates were loaded into Bio-Spin chromatography columns (Bio-Rad Laboratories #732-6008) loaded with Strep-Tactin sepharose (400 µl 50% slurry; IBA Lifesciences #2-1201-010) and washed with ice-cold PLCLB lysis buffer and ice-cold PLCLB buffer without Triton X-100 and protease inhibitors. Bound proteins were eluted twice with 300 µl of freshly prepared 0.5 mM biotin in PLCLB buffer without Triton X-100 and protease inhibitors. Liquid chromatography–tandem mass spectrometry analysis was

performed as described previously (24). Two biological replicates were used.

Luciferase assay

SW1222 cells transduced with lentivirus were trypsinized and 100,000 cells were plated into wells of a 24 well plate. Cells were transfected with 1 µg of *NOTCH1* promoter-based luciferase reporter (N1PR-luc) using Fugene6 transfection agent according to manufacturer's instructions (Promega #E2692) and lysed 48 h later. Luciferase measurement was done using the dual firefly luciferase assay kit and preformed according to manufacturer's instruction (Promega #E1910). All experiments were done in quadruplicate and repeated 2-3 times. Luciferase value was normalized to protein concentration.

Gene editing with the CRISPR/Cas9 system

Four different guide RNAs (gRNAs) targeting *PROX1* start codon region were designed using http://crispr.mit.edu/ (gPROX1.1: GCTCAAGAATCCCGGGACCCTGG, gPROX1.2: ATCTTCAAAAGCTCGTCAGCTGG, gPROX1.3: CCTGAGAGCAAAGCGCGCCCGGG, gPROX1.4: CGGGTTGAGAATATAATTCGGGG). gRNA-PCR transcriptional units were assembled as previously described (25) and tested by transfection to HEK293 cells together with WT SpCas9 expressing plasmid CAG-Cas9-T2A-EGFP-ires-puro (Addgene plasmid #78311). Deletion generation was assessed by PCR of the targeted region (PROX1_Fw: GTGCCATAAATCCCAGAGCCTATG, PROX1_Rv: ACTTTCTCGGGGACTCACAGAC). gRNAs pairs (1+3 and 1+4) generating deletions most efficiently were cloned into a modified version of LentiCRISPR v2 backbone (Addgene plasmid #52961). SW1222 cells were transduced with lentivirus containing the sgPROX1-1 (gRNA pair 1+3), sgPROX1-2 (gRNA pair 1+4) or sgCTRL constructs and selected using 5 µg/ml puromycin (Merck #540222-100). The cells were then used for further experiments. PROX1 deletion was confirmed by western blot.

Microarray experiments and Gene Set Enrichment Analysis

The quality of RNA was determined with Bioanalyzer (Agilent Technologies) and further analyzed on genome-wide Illumina Mouse WG-6 v2 Expression BeadChips (Illumina). Illumina's GenomeStudio software was used for initial data analysis and quality control and the detailed data analysis was performed with the Chipster software (www.chipster.csc.fi). The data were normalized with quantile normalization. When comparing the expression profiles of TdTomato+ and TdTomato- organoids, the datasets derived from hybridizations at different time points were normalized separately with quantile and gene average normalizations and the data were then unified. For pathway enrichment analysis, the Enrichr software (http://amp.pharm.mssm.edu/Enrichr/) was used. The gene expression dataset was transferred to the Gene Set Enrichment Analysis software (http://www.broadinstitute.org/gsea) (26, 27) and the analysis was carried out with default parameters except that the „exclude smaller sets" was set to 25 and gene permutation was applied. We used a modified list of the kegg.v3.1.symbols gene set (http://www.broadinstitute.org/gsea/msigdb) with the addition intestinal stem cell-specific genes (28), genes activated during $Apc^{min/+}$ tumorigenesis and suppressed by Notch1 activation, and genes upregulated in Notch1-activated tumors (12). FDR q-value<0.1 was regarded significant. The microarray data can be accessed from the Gene Expression Omnibus under the accession number GSE117981.

Statistical Analysis

Data are presented as mean+SEM unless otherwise indicated. Statistical comparison of two groups was done by two-tailed unpaired t-test using the GraphPad Prism 6.0 software. $P<0.05$ was considered statistically significant and the significance is marked by *$P<0.05$, **$P<0.01$ and ***$P<0.005$.

Other methods are detailed in the Supplementary Materials and Methods.

Results

Notch activity is essential for intestinal tumor development during a transient phase after *Apc* deletion. NOTCH1 was previously reported to suppress PROX1 expression in intestinal adenoma cells (12). In order to study this process in adenoma stem cells, we established organoids derived from *Apc$^{flox/flox}$; Lgr5-EGFP-IRES-Cre^{ERT2}* (LApc) or *Apc$^{flox/flox}$*; *Villin-Cre^{ERT2}* (VApc) mice. For induction of tumorigenesis, 4-OH-Tam was added to the organoid cultures, leading to *Apc* deletion only in the LGR5+ intestinal stem cells (LApc$^{\Delta/\Delta}$) or in all intestinal epithelial cells (VApc$^{\Delta/\Delta}$). To model the effect of Notch inhibition after *Apc* deletion, we inhibited Notch by adding the γ-secretase inhibitor (GSI) DBZ or DAPT to the cultures three days later (Fig. 1A). Notch inhibition decreased the number of viable organoids and RNAs encoding the Notch target genes hairy/enhancer of split (*Hes1*), Notch regulated ankyrin repeat protein (*Nrarp*) and Olfactomedin 4 (*Olfm4*), and the intestinal stem cell markers Leucine-rich repeat-containing G-protein coupled receptor 5 (*Lgr5*) and Achaete-Scute family BHLH transcription factor 2 (*Ascl2*) in both *Apc*-deleted and control organoids (Supplementary Fig. S1A and 1B). Lgr5-EGFP+ intestinal stem cell number was also decreased, indicating that Notch is critical for LGR5+ stem cell activity early after *Apc* deletion (Fig. 1B). Furthermore, Notch inhibition increased the expression of *Prox1* RNA and the number of PROX1+ cells (Fig. 1B and Supplementary Fig. S1A and 1B). Although the overall number of Lgr5-EGFP+ stem cells decreased, only a minor decrease of the Lgr5-EGFP+ PROX1+ cell population was observed (Fig. 1B**)**. Furthermore, single cell RNA analysis of DBZ or vehicle treated *Apc$^{flox/flox}$*; *villin-Cre^{ERT2}* organoids showed that the *Prox1* expressing cluster was enriched for intestinal stem cell markers *Lgr5* and *Tnfrsf19* (15, 29) after Notch inhibition (Fig. 1C). These data suggested that the PROX1+ stem-like cells had a selective growth advantage when Notch was inhibited.

Kinetic analysis of 4-OH-Tam treated *Apc$^{flox/flox}$*; *villin-Cre^{ERT2}* organoids revealed that increased expression of *Prox1* and the Wnt target genes *Axin2*, *Sox9*, *c-Myc* correlated with decreased expression of Notch targets *Olfm4* and *Hes1* (Fig. 2A-D). However, Notch inhibition on day 12 after *Apc* deletion

no longer affected the proportion of viable organoids, their colony formation efficiency, or the viability of patient-derived CRC organoids (Fig. 2E and 2F**)**, suggesting that active Notch signaling was no longer required to maintain *Apc* mutant intestinal epithelium. In agreement with this, the Lgr5-EGFP+ cells in the control intestine of *Apc$^{flox/flox}$; Lgr5-EGFP-IRES-Cre^{ERT2}* mice were uniformly positive for NICD1 (Fig. 2G**)**, whereas only 36% of the Lgr5-EGFP+ cells were positive for NICD1 21 days after *Apc* deletion (Fig. 2H). A majority of the Lgr5-EGFP + stem cells were PROX1+, and PROX1+ cells were negative for NICD1 (Fig. 2I and 2J), supporting the notion that PROX1+ cells have a selective growth advantage after *Apc* deletion. Collectively, these results suggest that the Notch pathway is important for intestinal stem cell activity during a transient phase after *Apc* deletion, but is inactivated in later appearing PROX1-expressing stem-like cells.

Chemical Notch inhibition provides the PROX1+ adenoma cells a growth advantage. To assess if the PROX1+ adenoma cells retain their stem cell activity even when Notch activity is inhibited, we induced tumorigenesis by tamoxifen treatment of *Apc$^{flox/flox}$; Lgr5-EGFP-IRES-Cre^{ERT2}* mice and applied the γ-secretase-inhibitor DBZ 5 days later for 5 days. As reported previously, DBZ treatment converted intestinal epithelial cells into Mucin2+ (MUC2) goblet cells and reduced the number of Lgr5-EGFP+ stem cells in the normal intestine (7), leading to death of the mice within 8 days after the start of the DBZ treatment. Although the number of Lgr5-EGFP+ adenoma stem cells was decreased at day 10 after *Apc* deletion when the Notch pathway was inhibited, the majority of them were PROX1+ (Fig. 3A and 3B**)**. In contrast, Notch inhibition starting 21 days after *Apc* deletion, when the majority of the Lgr5-EGFP+ cells were PROX1+, did not significantly decrease the number of Lgr5-EGFP+ stem cells (Fig 3C**)**. Furthermore, the MUC2+ goblet cells occurred selectively in the PROX1- tumor cell population (Fig. 3D-F and Supplementary Fig. S2A**)**. DBZ treatment also promoted increased proliferation of PROX1+ tumor cells and decreased proliferation of PROX1- cells on days 10 and 26 after *Apc* deletion (Fig. 3G-

I and Supplementary Fig. S2B), suggesting that Notch inhibition provides the PROX1+ cells an additional growth advantage.

To further analyze the PROX1+ stem-like cells, we induced lineage tracing in *Apc*$^{min/+}$*; Rosa26-*$^{LSL\text{-}TdTomato}$*; Prox1-Cre*^{ERT2} mice and treated the mice with DBZ or vehicle for 4 days. TdTomato fluorescence 3 days after the last dose of DBZ indicated that some PROX1+ cells had differentiated to PROX1-/TdTomato+ Paneth cells (lysozyme+) and goblet cells (MUC2+) (Supplementary Fig. S2C and S2D). Furthermore**,** Notch inhibition increased the number of proliferating PROX1+ tumor cells and the number of proliferating TdTomato labelled PROX1- progeny in more advanced tumors of the *Apc*$^{min/+}$ mice (Fig. 3J-L), suggesting that continued growth of the tumors originates from the PROX1+ tumor cells.

Induction of NOTCH1 reduces tumor stem cell activity. As PROX1+ adenoma cells retained their stem cell activity after Notch inhibition, we asked if NOTCH1 overexpression affects the stem cell properties of PROX1+ cells in mouse tumor organoid cultures and human CRC cells. We transduced *Apc*-mutant organoids derived from *Apc*$^{min/+}$*; Rosa26-*$^{LSL\text{-}TdTomato}$*; Prox1-Cre*^{ERT2} mice with NICD1-EGFP or control lentivirus and then subjected them to short-term genetic labeling by applying 4-OH-Tam. Sixteen hours after the addition of 4-OH-Tam, only cells positive for PROX1 displayed red TdTomato fluorescence (Fig. 4A and 4B), confirming the specificity of the labeling. The NICD1 overexpressing cells formed less colonies, which had fewer TdTomato+ cells than control lentivirus-transfected cells (Fig. 4C and 4D), reflecting *Prox1* suppression in these cells. NICD1 overexpression in the PROX1+ SW620 and SW1222 human CRC cell lines that are enriched for stem-like cells (30, 20) indicated that the NICD1 overexpressing cells suppressed *PROX1* RNA and protein (Fig. 4E-G), supporting previous findings (12). Furthermore, when the control and NICD1 transduced SW1222 cells were grown as three-dimensional cultures in Matrigel, the NICD1 overexpressing cells were unable to

form "megacolonies" (Fig. 4H**)**, indicating that they lack stem cell properties (31). These results suggest that NOTCH1 activation suppresses PROX1 and thus stem cell properties of PROX1+ CRC cells.

PROX1 regulates the Notch pathway in colorectal cancer. As increased *Prox1* expression correlated with decreased *Olfm4* and *Hes1* expression, we next assessed if PROX1 regulates the Notch pathway. We first analyzed the gene expression signature of FACS isolated TdTomato+/PROX1+ cells by microarray analysis. As expected (5), we found that *Prox1* expressing cells displayed an enrichment of the intestinal stem cell gene signature (28) (Supplementary Fig. S3A), which had similarity to gene sets upregulated by *Apc* mutation and suppressed by NICD1 overexpression in intestinal adenomas (12) (Supplementary Fig. S3B). Accordingly, the *Prox1* cell transcriptome showed a negative enrichment of genes induced by NICD1 overexpression (Supplementary Fig. S3C), indicating that Notch signaling is suppressed in the *Prox1* expressing cells.

We next induced *Prox1* and *Apc* deletion by tamoxifen treatment of $Apc^{flox/flox}$; $Prox1^{flox/flox}$; *Lgr5-EGFP-IRES-*Cre^{ERT2} ($LApcP^{\Delta/\Delta}$) mice to analyze PROX1 regulation of the Notch pathway in intestinal adenoma stem cells. Interestingly, *Prox1* deletion increased the ratio of OLFM4+ cells in the Lgr5-EGFP+ cell population, suggesting Notch activation in these cells (Fig. 5A and 5B). Also, *Prox1* deletion in organoids derived from $Apc^{min/+}$; $Prox1^{flox/flox}$; *villin-*Cre^{ERT2} *mice* resulted in increased expression of the Notch targets *Olfm4* and *Hey2* (Fig. 5C). Furthermore, *Prox1* deletion decreased the expression of Pleiotrophin (*Ptn*), Pyruvate dehydrogenase kinase 4 (*Pdk4*) and Distal-less homebox 3 (*Dlx3*), genes that are suppressed by NICD1 overexpression, and increased the expression of Tripartite motif-containing protein 31 (*Trim31*) and Carbonic anhydrase 13 (*Car13*), transcripts that are induced by NICD1 in intestinal adenomas (12) (Supplementary Fig. S3D).

In order to explore PROX1 regulation of NOTCH in human CRC, we employed CRISPR/Cas9 to delete *PROX1* exon 2 (Supplementary Fig. S3E and S3F). SW1222 cells were lentivirally transduced with Cas9 plus two different PROX1 gRNAs and selected with puromycin. PROX1 deletion was first confirmed by western blotting (Supplementary Fig. S3G), and the cells were then transfected with a *NOTCH1*-promoter driven luciferase reporter. When analyzed 48 h later, the PROX1 deleted cells showed a two-fold higher luciferase signal than the control cells (Fig. 5D). Furthermore, PROX1 deletion increased expression of the Notch targets *OLFM4* and *HEY2* (Fig. 5E). PROX1 overexpression in the NOTCH1 active LS174T cells (8) also decreased the expression of *OLFM4* and *HEY2* (Fig. 5F). These data indicate that PROX1 suppresses the Notch pathway in mouse adenomas and human CRC cells.

PROX1 recruits the NuRD complex to suppress the Notch pathway. To investigate the mechanism of how PROX1 suppresses the Notch pathway, we performed BirA-mediated proximity labeling to identify PROX1 interacting proteins in SW1222 cells (Supplementary Fig. S4A and S4B). Remarkably, we found that PROX1 interacts with several proteins that have chromatin remodeling function. In particular, several components of the NuRD corepressor complex were among the top 10 hits (Supplementary Table S1). By co-immunoprecipitation, we determined that at least HDAC1 and MTA1, key components of the complex, co-precipitated with PROX1 from lysates of SW1222 and SW620 cells (Fig. 6A). The prior report that the NuRD complex suppresses Notch pathway in Schwann cells (32), raised the possibility that PROX1 suppresses the Notch pathway in CRC cells via the NuRD complex. To assess this, we treated SW1222 cells with two HDAC inhibitors for 72 hours to inhibit HDAC1 and HDAC2. This increased the expression of the Notch target genes *OLFM4* and *HEY2* (Supplementary Fig. S4C). Lentiviral silencing of HDAC1, HDAC2 or MTA1 increased the *NOTCH1* promoter-luciferase reporter expression and the expression of *OLFM4* (Fig. 6B-E and Supplementary Fig. S4D-F), indicating that the NuRD complex suppresses Notch signaling in CRC. Furthermore, HDAC1, HDAC2 or MTA1 silencing in PROX1 overexpressing LS174T cells blocked the PROX1-mediated

suppression of *OLFM4* (Fig 6F), suggesting that PROX1 acts via the NuRD complex to regulate the Notch signaling pathway in CRC. Chromatin immunoprecipitation (ChIP) using antibodies against PROX1, HDAC1 and MTA1 followed by qPCR of three regions of the *NOTCH1* promoter revealed two potential PROX1 binding sites at -1.5kb and -0.8kb, whereas MTA1 bound weakly to the *NOTCH1* promoter at -3.5kb (Fig. 6G-I and Supplementary Fig. S4G**)**. These data indicate that PROX1 suppresses the Notch pathway by recruiting the NuRD complex to the *NOTCH1* promoter (Fig. 6J).

Discussion

In this study, we provide evidence that the PROX1 transcription factor regulates CRC stem-like cells via a bidirectional interaction with the Notch pathway. We show that Notch inhibition in *Apc* wild type or mutant organoids decreases expression of intestinal stem cell markers while increasing PROX1+ cells. Chemical Notch inhibition provided PROX1+ cells a further growth advantage in the emerging tumors. Interestingly, *Prox1* deletion increased expression of Notch target genes and *NOTCH1* promoter activity. Mechanistic analysis of this finding indicated that PROX1 recruits the NuRD complex to the *NOTCH1* promoter to suppress the Notch pathway in CRC.

Intestinal crypt cells are plastic and compensatory mechanisms have been reported to produce fast-cycling crypt base columnar stem cells following injury have been reported (33-35). Similarly, colorectal tumors are composed of a flexible hierarchy of stem-like cells, progenitors and more differentiated cells (reviewed in 36). In the normal intestine, PROX1 is expressed in enteroendocrine cells and some Paneth cells (3, 5). Furthermore, the PROX1+ enteroendocrine cells can function as injury-inducible stem cells (35). In CRC, PROX1 is directly regulated by the β-catenin/TCF4 pathway. Notch inhibition at an early phase after *Apc* deletion resulted in increased production of PROX1+ adenoma cells, but Notch inhibition

had only a minor effect later during tumor development due to Notch downregulation in PROX1+ cells. Analysis of single cell RNA sequencing of control and Notch inhibited organoids showed that *Prox1*+ cell clusters express some intestinal stem cell markers, suggesting that the PROX1+ cells form a subpopulation of intestinal stem-like cells. Furthermore, the LGR5+PROX1- cells were decreased by Notch inhibition indicating that a subpopulation of the stem-like cells is Notch dependent. In line with this, Schmidt and colleagues demonstrated that high NOTCH activity marks a distinct colon cancer subpopulation with low levels of WNT and MAPK activity (37). Furthermore, NOTCH1 was shown to be co-expressed with the intestinal stem cell marker BMI1, whereas the LGR5+ stem-like cells expressed Wnt markers (38). Considering that PROX1 is a Wnt target, these studies suggest that PROX1 marks a high Wnt and Notch negative stem-like cell population.

NOTCH1 is known to suppress PROX1 expression in lymphatic endothelial cells (39), thyroid cancer cells (40), myoblasts (41), in the developing *Drosophila intestine* (42) and in mouse intestinal adenomas (12). Although the function of the Notch pathway in the WT intestinal stem cells is well established (8), how it affects CRC progression is unclear. NOTCH1 has been shown to be essential in the initiation of CRC (7, 11, 12). However, deletion of the Notch effector *Rbpj* did not affect tumorigenesis in *Apc* mutant intestine (43). Furthermore, aberrant NOTCH1 expression decreases during tumor progression and metastasis, suggesting that the Notch pathway functions mainly in the early phase of CRC progression (44). On the other hand, PROX1 was shown to be important in CRC progression and metastatic outgrowth of Wnt high colon cancer cells (3, 45), rather than for adenoma initiation. In our models, PROX1 and the Notch pathway suppressed each other, indicating that high PROX1 expression and active Notch signaling are mutually exclusive. PROX1 has previously been shown to suppress the Notch pathway to allow differentiation of myoblasts (41) and neurons (46). We show evidence that PROX1 suppresses Notch pathway in CRC via recruiting the NuRD complex to the *NOTCH1* promoter. The

NuRD complex consists of seven subunits that function together in chromatin remodeling and histone deacetylation (reviewed in ref. 47). Previous studies have shown that the NuRD complex maintains the silencing of tumor suppressor genes in CRC (48). Furthermore, deficiency of Mbd2, a component of the complex, reduces tumor burden in *Apc*$^{min/+}$ mice and attenuates Wnt signaling (49, 50). These studies indicate that the NuRD complex performs an important function in CRC. Importantly, aberrant NOTCH1 expression suppressed the stem cell activity of the PROX1 positive stem-like cells. These observations raise the possibility that PROX1 suppresses the Notch pathway to promote malignant growth.

In conclusion, we demonstrate that PROX1 interacts with the NuRD complex to suppress Notch signaling in CRC stem-like cells. Furthermore, we show that ectopic expression of active NOTCH1 suppresses PROX1 and the stem cell activity of PROX1 positive cells, suggesting a reciprocal interaction of PROX1 and Notch pathways in regulation of CRC stem-like cells. Based on our results, we propose a model where the LGR5+ stem cells require active Notch signaling early after *Apc* deletion. However, some of these cells start to express PROX1, which then suppresses the Notch pathway. These PROX1+ LGR5+ cells proliferate and support tumor growth independently of the Notch pathway. Our studies thus give new insight into the complex regulation of stem-like cells and identify PROX1 as a marker of a Notch independent stem cell population.

Acknowledgments: This work was funded by the Academy of Finland (grants n:o 292816 and 273817, Centre of Excellence Program 2014-2019: Translational Cancer Biology grant n:o 307366), Cancer Foundation in Finland, Sigrid Juselius Foundation, Hospital District of Helsinki and Uusimaa Research Grants, Helsinki Institute of Life Sciences (HiLIFE), Biocenter Finland (all to K. Alitalo), Swedish cultural foundation in Finland, Magnus Ehrnrooth foundation, Biomedicum Helsinki foundation, Ida Montini foundation, K Albin Johansson foundation, Orion research foundation, Medicinska understödsföreningen Liv&Hälsa and Maud Kuistila memorial foundation (all to J. Högström), János

Bolyai Grant by the Hungarian Academy of Sciences (to Z. Wiener). We thank Dr Markku Varjosalo and the proteomics unit at the Institute of Biotechnology, University of Helsinki, for performing mass spectromerty, Dr. Seppo Kaijalainen for cloning the BirA-PROX1 construct, Dr. Timo Otonkoski from the Molecular Neurology Program and Biomedicum Stem Cell Center, University of Helsinki for supporting the cloning of the sgCTRL and sgPROX1 constructs, Dr Guillermo Oliver from the Feinberg Cardiovascular Research Institute, Northwestern University, Chicago for the *Prox1*$^{flox/flox}$ and *Prox1-Cre*^{ERT2} mice; Dr. Tohru Kiyono from the National Cancer Center, Japan for the NOTCH1 promoter-based luciferase reporter, Dr. Riikka Kivelä for discussions, Drs. Pekka Katajisto, Saara Ollila and Cecilia Sahlgren for reading and commenting of the manuscript, and David He, Kirsi Mattinen, Tanja Laakkonen and Tapio Tainola for technical assistance. We also thank the Single Cell Analytics core facility at the Institute for Molecular Medicine Finland, the Biomedicum functional genomics unit and Biomedicum imaging unit, University of Helsinki for providing material and services

References

1. Fearon ER, Vogelstein B. A genetic model for colorectal tumorigenesis. Cell 1990;61:759-67.

2. Gregorieff A, Clevers H. Wnt signaling in the intestinal epithelium: From endoderm to cancer. Genes Dev 2005;19:877-90.

3. Petrova TV, Nykänen A, Norrmén C, Ivanov KI, Andersson LC, Haglund C, et al. Transcription factor PROX1 induces colon cancer progression by promoting the transition from benign to highly dysplastic phenotype. Cancer cell 2008;13:407-19

4. Elsir T, Smits A, Lindström MS, Nistér M. Transcription factor PROX1: Its role in development and cancer. Cancer Metastasis Rev 2012;31:793-805.

5. Wiener Z, Högström J, Hyvönen V, Band AM, Kallio P, Holopainen T, et al. Prox1 promotes expansion of the colorectal cancer stem cell population to fuel tumor growth and ischemia resistance. Cell reports 2014;8:1943-56

6. Elyada E, et al. CKIalpha ablation highlights a critical role for p53 in invasiveness control. Nature 2011;470:409-13.

7. Fre S, Pallavi SK, Huyghe M, Lae M, Janssen KP, Robine S, et al. Notch and wnt signals cooperatively control cell proliferation and tumorigenesis in the intestine. Proc Natl Acad Sci U S A 2009;106:6309-14.

8. Tian H, Biehs B, Chiu C, Siebel CW, Wu Y, Costa M, et al. Opposing activities of notch and wnt signaling regulate intestinal stem cells and gut homeostasis. Cell reports 2015;11:33-42.

9. Pellegrinet L, Rodilla V, Liu Z, Chen S, Koch U, Espinosa L, et al. Dll1-and dll4-mediated notch signaling are required for homeostasis of intestinal stem cells. Gastroenterology 2011;140:1230,1240.

10. van Es JH, van Gijn ME, Riccio O, van den Born M, Vooijs M, Begthel H, et al. Notch/γ-secretase inhibition turns proliferative cells in intestinal crypts and adenomas into goblet cells. Nature 2005;435:959-63.

11. Rodilla V, Villanueva A, Obrador-Hevia A, Robert-Moreno A, Fernandez-Majada V, Grilli A, et al. Jagged1 is the pathological link between wnt and notch pathways in colorectal cancer. Proc Natl Acad Sci U S A 2009;106:6315-20.

12. Kim HA, Koo BK, Cho JH, Kim YY, Seong J, Chang HJ, et al. Notch1 counteracts WNT/beta-catenin signaling through chromatin modification in colorectal cancer. J Clin Invest 2012;122:3248-59.

13. Shibata H, Toyama K, Shioya H, Ito M, Hirota M, Hasegawa S, et al. Rapid colorectal adenoma formation initiated by conditional targeting of the apc gene. Science 1997;278:120-3.

14. Harvey NL, Srinivasan RS, Dillard ME, Johnson NC, Witte MH, Boyd K, et al. Lymphatic vascular defects promoted by Prox1 haploinsufficiency cause adult-onset obesity. Nat Genet 2005;37:1072-81.

15. Barker N, Van Es JH, Kuipers J, Kujala P, Van Den Born M, Cozijnsen M, et al. Identification of stem cells in small intestine and colon by marker gene Lgr5. Nature 2007;449:1003-7.

16. Srinivasan RS, Dillard ME, Lagutin OV, Lin FJ, Tsai S, Tsai MJ, et al. Lineage tracing demonstrates the venous origin of the mammalian lymphatic vasculature. Genes Dev 2007;21:2422-32.

17. Sato T, Stange DE, Ferrante M, Vries RG, Van Es JH, Van den Brink S, et al. Long-term expansion of epithelial organoids from human colon, adenoma, adenocarcinoma, and barrett's epithelium. Gastroenterology 2011;141:1762-72.

18. El Marjou F, Janssen K, Hung-Junn Chang B, Li M, Hindie V, Chan L, et al. Tissue-specific and inducible Cre-mediated recombination in the gut epithelium. Genesis 2004;39:186-93.

19. Sato T, Vries RG, Snippert HJ, Van De Wetering M, Barker N, Stange DE, et al. Single Lgr5 stem cells build crypt villus structures in vitro without a mesenchymal niche. Nature 2009;459:262-5.

20. Ashley N, Yeung T, Bodmer WF. Stem Cell Differentiation and Lumen Formation in Colorectal Cancer Cell Lines and Primary Tumours. *Cancer Res* 2013;73:5798-809.

21. Butler A, Hoffman P, Smibert P, Papalexi E, Satija R. Integrating single-cell transcriptomic data across different conditions, technologies, and species. Nat Biotechnol 2018;36:411.

22. Yugawa T, Handa K, Narisawa-Saito M, Ohno S, Fujita M, Kiyono T. Regulation of Notch1 gene expression by p53 in epithelial cells. *Mol Cell Biol* 2007;27:3732-42.

23. Roux KJ, Him DI, Raifa M, Burke B. A promiscuous biotin ligase fusion protein identifies proximal and interacting proteins in mammalian cells. *J Cell Biol* 2012;196:801-10.

24. Yadav L, Tamane F, Göös H, van Drogen A, Katainen R, Aebersold R, *et al.* Systematic analysis of human protein phosphatase interactions and dynamics. *Cell Syst* 2017;4:430-444.

25. Balboa D, Weltner J, Eurola S, Trokovic R, Wartiovaara K, Otonkoski T. Conditionally stabilized dCas9 activator for controlling gene expression in human cell reprogramming and differentiation. Stem cell reports 2015;5:448-59.

26. Mootha VK, Lindgren CM, Eriksson K, Subramanian A, Sihag S, Lehar J, et al. PGC-1α-responsive genes involved in oxidative phosphorylation are coordinately downregulated in human diabetes. Nat Genet 2003;34:267-73.

27. Subramanian A, Tamayo P, Mootha VK, Mukherjee S, Ebert BL, Gillette MA, et al. Gene set enrichment analysis: A knowledge-based approach for interpreting genome-wide expression profiles. Proc Natl Acad Sci U S A 2005;102:15545-50

28. van der Flier, Laurens G, van Gijn ME, Hatzis P, Kujala P, Haegebarth A, Stange DE, et al. Transcription factor achaete scute-like 2 controls intestinal stem cell fate. Cell 2009;136:903-12.

29. Fafilek B, Krausova M, Vojtechova M, Pospichalova V, Tumova L, Sloncova E, et al. Troy, a tumor necrosis factor receptor family member, interacts with lgr5 to inhibit wnt signaling in intestinal stem cells. Gastroenterology 2013;144:381-91.

30. Wang C, Xie J, Guo J, Manning HC, Gore JC, Guo N. Evaluation of CD33 and CD133 as cancer stem cell markers for colorectal cancer. *Oncol Rep* 2012;28:1301-8.

31. Yeung TM, Gandhi SC, Wilding JL, Muschel R, Bodmer WF. Cancer stem cells from colorectal cancer-derived cell lines. *Proc Natl Acad Sci U S A* 2010;107:3722-7.

32. Wu LM, Wang J, Conidi A, Zhao C, Wang H, Ford Z, *et al.* Zeb2 recruits HDAC-NuRD to inhibit Notch and controls Schwann cell differentiation and remyelination. *Nat Neurosci* 2016 ;19:1060-72.

33. Tian H, Biehs B, Warming S, Leong KG, Rangell L, Klein OD, et al. A reserve stem cell population in small intestine renders Lgr5-positive cells dispensable. Nature 2011;478:255.

34. Tetteh PW, Basak O, Farin HF, Wiebrands K, Kretzschmar K, Begthel H, et al. Replacement of lost Lgr5-positive stem cells through plasticity of their enterocyte-lineage daughters. Cell Stem Cell 2016;18:203-13.

35. Yan KS, Gevart O, Zheng GXY, Anchang B, Probert CS, Larkin KA *et al.* Intestinal enteroendocrine lineage cells possess homeostatic and injury-inducible stem cell activity. *Cell Stem cell* 2017;21:78-90.

36. Stange DE, Clevers H. Concise review: the yin and yang of intestinal (cancer) stem cells and their progenitors. *Stem Cells* 2013;31:2287-95.

37. Schmidt EM, Lamprecht S, Blaj C, Schaaf C, Krebs S, Blum H, et al. Targeting tumor cell plasticity by combined inhibition of NOTCH and MAPK signaling in colon cancer. J Exp Med 2018;215:1693-708.

38. Srinivasan T, Walters J, Bu P, Than EB, Tung KL, Chen KY, et al. NOTCH signaling regulates asymmetric cell fate of fast- and slow-cycling colon cancer-initiating cells. Cancer Res 2016;76:3411-21.

39. Kang J, Yoo J, Lee S, *et al*. An exquisite cross- control mechanism among endothelial cell fate regulators directs the plasticity and heterogeneity of lymphatic endothelial cells. *Blood* 2010;116: 140-150.

40. Choi D, Ramu S, Park E, Jung E, Yang S, Jung W, *et al*. Aberrant activation of Notch signaling inhibits PROX1 activity to enhance the malignant behavior of thyroid cancer cells. *Cancer Res* 2016;76:582-93.

41. Kivelä R, Salmela I, Nguyen YH, Petrova TV, Koistinen HA. Wiener Z, *et al.* The Transcription factor Prox1 is essential for satellite cell differentiation and muscle fiber-type regulation. *Nat Commun* 2016;7:13124.

42. Guo Z and Ohlstein B. Bidirectional Notch signaling regulates Drosophila intestinal stem cell multipotency. *Science* 201520:350(6263).

43. Peignon G, Durand A, Cacheux W, Ayrault O, Terris B, Laurent-Puig P, et al. Complex interplay between beta-catenin signalling and notch effectors in intestinal tumorigenesis. Gut 2011;60:166-76.

44. Veenendaal LM, Kranenburg O, Smakman N, Klomp A, Borel Rinkes IH, van Diest PJ. Differential notch and TGFβ signaling in primary colorectal tumors and their corresponding metastases. Analytical Cellular Pathology 2008;30:1-11.

45. Ragusa S, Cheng J, Ivanov KI, Zangger N, Ceteci F, Bernier-Latmani J, et al. PROX1 promotes metabolic adaptation and fuels outgrowth of wnt high metastatic colon cancer cells. Cell reports 2014;8:1957-73.

46. Kaltezioti V, Kouroupi G, Oikonomaki M, Mantouvalou E, Stergiopoulos A, Charonis A, *et al.* Prox1 regulates the Notch1-mediated inhibition of neurogenesis. *PLoS Biol* 2010;21:8 e1000565

47. Lai AY and Wade PA. NuRD: A multi-faceted chromatin remodeling complex in regulating cancer biology. *Nat Rev Cancer* 2011;11: 588-59

48. Cai Y, Geutjes EJ, de Lint K, Roepman P, Bruurs L, Yu LR, *et al*. The NuRD complex cooperates with DNTMs to maintain silencing of key colorectal tumor suppressor genes. *Oncogene* 2014;33:2157-68

49. Sansom OJ, Berger J, Bishop SM, Hendrich B, Bird A, Clarke AR. Deficiency of Mbd2 suppresses intestinal tumorigenesis. *Nat Genet* 2003;34:145-7.

50. Phesse TJ, Parry L, Reed KR, Ewan KB, Dale TC, Sansom OJ *et al*. Deficiency of Mbd2 attenuates Wnt signaling. *Mol Cell Biol* 2008;28:6094-103

Figure legends

Figure 1. Notch activity is essential for the maintenance of intestinal stem cells during a transient phase after *Apc* deletion. A) Schematic illustration of the experimental design. B) Quantification of Lgr5-EGFP+ and PROX1+ cells based on flow cytometry of Lgr5-EGFP fluorescence and PROX1 immunostaining *in* $LApc^{\Delta/\Delta}$ d8 organoids. C) RNA expression analysis of *Prox1*, *Lgr5* and *Tnfrsf19* expressing single cells in $Apc^{flox/flox}$; $Villin\text{-}Cre^{ERT2}$ d8 organoids. Feature heatmap and t-SNE plot was used to visualize clustering of RNA sequenced single cells. Organoids were treated for 5 days with the

γ-secretase inhibitor DBZ, starting on day three after the addition of 4-OH-Tam. Student's unpaired t-test, n=3+3, *P<0.05.

Figure 2. *Prox1* induction correlates with decreased Notch target gene expression after *Apc* deletion. A-D) Kinetic analysis of RNA encoding *Prox1* (A), the Wnt target genes *Axin2*, *Sox9* and *c-Myc* (B), and Notch-targets *Olfm4* (C) and *Hes1* (D) after *Apc* deletion in the $Apc^{flox/flox}$; *villin-*Cre^{ERT2} organoids. E) The ratio of viable organoids, and number of new colonies after re-plating of DAPT treated $Apc^{flox/flox}$; *Lgr5-EGFP-IRES-*Cre^{ERT2} ($LApc^{\Delta/\Delta}$) organoids. The treatment was started 12 days after *Apc* deletion for five days. F) The percentage of viable organoids in DBZ treated patient-derived CRC organoids. G-H) Immunofluorescence staining of Lgr5-EGFP and NICD1 in $Apc^{flox/flox}$; *Lgr5-EGFP-IRES-*Cre^{ERT2} intestine before (G) and 21 days (H) after *Apc* deletion. Note that whereas all EGFP+ cells are NICD1+ in the control crypt, only some Lgr5-EGFP+ cells are NICD1+ in the adenomas. I-J) Lgr5-EGFP, NICD1 and PROX1 immunofluorescence in $Apc^{flox/flox}$; *Lgr5-EGFP-IRES-*Cre^{ERT2} intestines 21 days after tamoxifen administration. Note that PROX1+ Lgr5-EGFP+ cells are negative for NICD1. Arrowheads mark NICD1+ cells. Student's unpaired t-test, n=3+3. Scale bars= 20 μm.

Figure 3. Chemical Notch inhibition provides the PROX1+ adenoma cells a growth advantage. A-C) Lgr5-EGFP and PROX1 immunostaining (A) and quantification of PROX1+ and PROX1- Lgr5-EGFP+ cells (B-C) in *Apc* deleted $Apc^{flox/flox}$; *Lgr5-EGFP-IRES-*Cre^{ERT2} intestines treated with the γ-secretase inhibitor DBZ. Arrowheads mark the Lgr5-EGFP+ cells. D-F) Goblet cell (MUC2) and PROX1 immunostaining (D) and quantification of PROX1+ and PROX1- MUC2+ tumor cells (E-F) in the same intestine. Arrowheads mark MUC2+ cells. G-I) EdU and PROX1 immunostaining (G) and quantification of PROX1+ and PROX1- EdU+ tumor cells (H-I) in the same intestine. Arrowheads mark PROX1+EdU+ cells. DBZ treatment was started on d5 (A,B,D,E,G,H) or d21 (C, F, I) after the addition of tamoxifen. J-L) EdU, TdTomato and PROX1 immunostaining (J) and quantification (K) of PROX1

negative EdU+ and EdU- cells derived from the PROX1 positive cells (TdTomato+) and total percentage of EdU+ cells (L) in tumors of *Apc*$^{min/+;}$ Rosa26$^{LSL\text{-}tdTomato}$*; Prox1-Cre*^{ERT2} mice treated with DBZ. Analysis was performed three days after the last injection of DBZ. Arrowheads mark TdTomato+/EdU+/PROX1- cells. Mice were given four (J-L) or five (A-I) i.p injections of DBZ (20 µmol/kg/day). EdU (1 mg/kg) was administered four hours prior to termination. Student's unpaired t-test, n=10-14, *P<0.05, **P<0.01. Scale bars= 20 µm.

Figure 4. Induction of NOTCH1 reduces tumor stem cell activity. A-B) Immunofluorescence image of an organoid (A) and flow cytometry (B) of PROX1 staining and TdTomato signals in single cells derived from *Apc*$^{min/+;}$ Rosa26$^{LSL\text{-}tdTomato}$*; Prox1-Cre*^{ERT2} organoids 16 h after addition of 4-OH-Tam. C) Comparison of the relative numbers of single cell-derived GFP control vs. NICD1-GFP colonies among *Apc*$^{min/+;}$ Rosa26$^{LSL\text{-}tdTomato}$*; Prox1-Cre*^{ERT2} organoids. D) Comparison of the relative number of GFP control and NICD1-GFP colonies among the tdTomato+ colonies. E-G) NICD1-GFP and PROX1 immunofluorescence staining (E), PROX1 RNA (F) and the ratio of GFP+/PROX1- cells (G) in SW1222 and SW620 cells four days after lentiviral transduction of GFP control or NICD1-GFP. Note that the NICD1+ cells are PROX1- (arrowheads). H) Images of colonies formed by SW1222 cells transduced with NICD1-GFP and GFP control lentiviruses. Note that NICD1-transduced cells fail to form colonies with multiple lumens. Student's unpaired t-test was used, *P<0.05, **P<0.01, ***P<0.005. Scale bars= 20 µm (E) or 100 µm (H).

Figure 5. Prox1 suppresses the Notch1 signaling pathway. A-B) Representative image of Lgr5-GFP fluorescence and OLFM4 and PROX1 immunostaining (A) and quantification of the ratio of PROX1+OLFM4-, PROX1-OLFM4+, PROX1+OLFM4+ and PROX1-OLFM4- Lgr5-EGFP+ cells (B) in adenomas derived from *Apc*$^{flox/flox}$*; Lgr5-EGFP-IRES-Cre*^{ERT2} (*LApc*$^{\Delta/\Delta}$) and *Apc*$^{flox/flox}$*; Prox1*$^{flox/flox}$*; Lgr5-EGFP-IRES-Cre*^{ERT2} (*LApcP*$^{\Delta/\Delta}$) mice 21 days after addition of Tam. C) RNA expression of Notch

target genes in *Apc*$^{min/+}$ (Ctrl) and *Apc*$^{min/+}$*; Prox1*$^{flox/flox}$*; villin-Cre*^{ERT2} (*Prox1*$^{\Delta/\Delta}$) organoids three days after addition of 4-OH-Tam. D-E) *NOTCH1* promoter-driven luciferase assay (D) and RNA expression of Notch target genes (E) in SW1222 cells transduced with sgCTRL or sgPROX1 lentiviruses. F) RNA expression of *PROX1* and NOTCH1 target genes in LS174T cells transduced with CTRL or PROX1 overexpressing lentivirus. Data is presented as fold change, mean+SD (C-F), n=4+4, Student's unpaired t-test, *P<0.05, **P<0.01, ***P<0.005. Scale bars= 20 µm.

Figure 6. Implication of the PROX1-NuRD corepressor complex in suppression of the NOTCH pathway. A) Co-immunoprecipitation of HDAC1 and MTA1 with PROX1 from lysates of SW1222 and SW620 cells. B-E) *NOTCH1* promoter-luciferase assay (B) and expression of OLFM4 RNA in SW1222 cells transduced with shSCR, shHDAC1 (C), shHDAC2 (D) or shMTA1 (E) lentivirus. F) Expression of *OLFM4* RNA in LS174T cells expressing CTRL or PROX1 lentivirus and transfected with shSCR, shHDAC1, shHDAC2 or shMTA1. G-I) Chromatin immunoprecipitation of PROX1, HDAC1 and MTA1 in SW620 cells, followed by RT-qPCR of three regions of the *NOTCH1* promoter. J) Schematic presentation of the PROX1-NuRD complex mediated suppression of the NOTCH1. Data is presented as fold change, mean+SD (B-F) or percentage of Input (G-I), n=4+4 (B-F), 2+2 (G-I), Student's unpaired t-test, *P<0.05, **P<0.01, ***P<0.005.

Author Manuscript Published OnlineFirst on August 28, 2018; DOI: 10.1158/0008-5472.CAN-18-0451
Author manuscripts have been peer reviewed and accepted for publication but have not yet been edited.

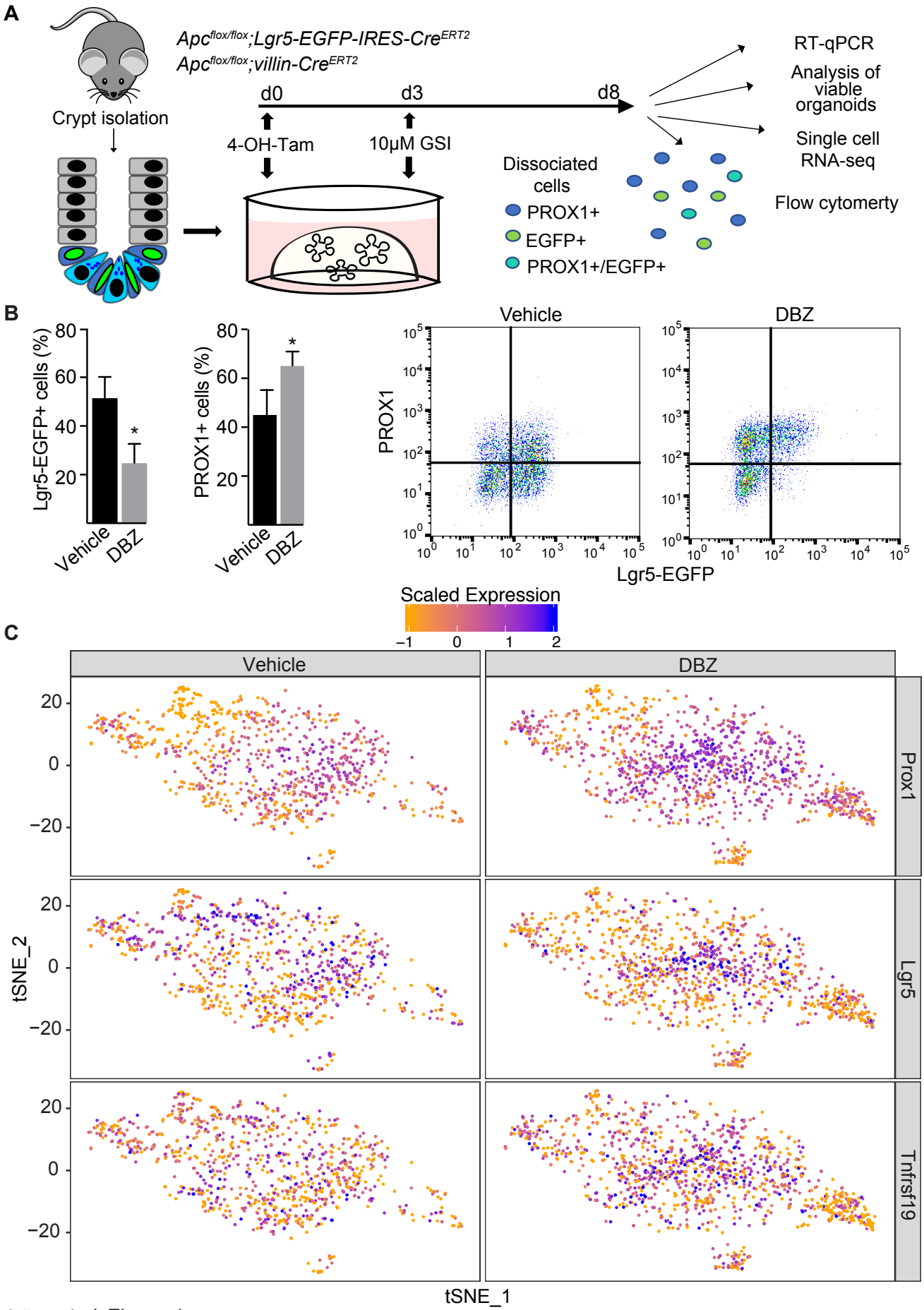

Högström *et al.* Figure 1

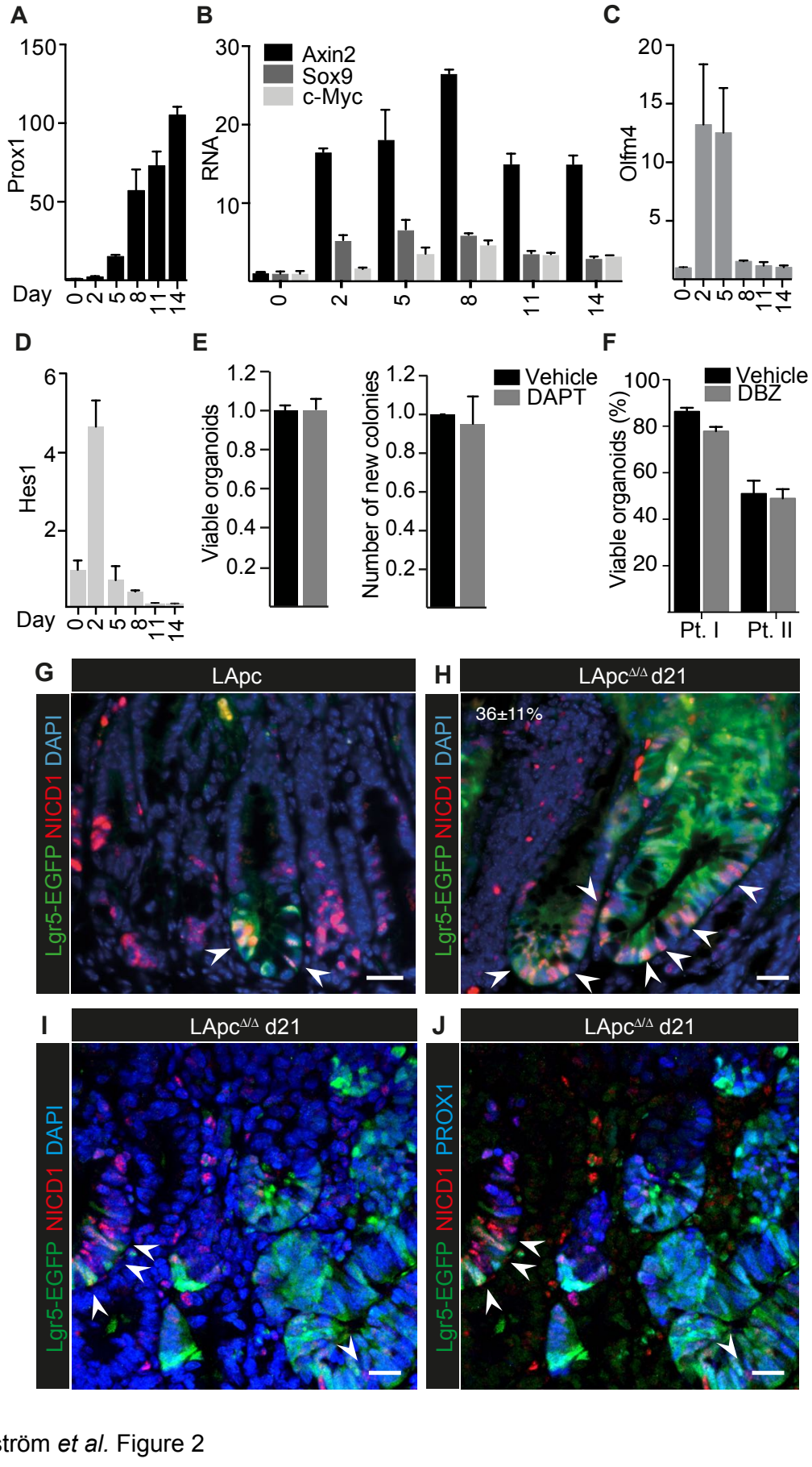

Högström *et al.* Figure 2

Author Manuscript Published OnlineFirst on August 28, 2018; DOI: 10.1158/0008-5472.CAN-18-0451
Author manuscripts have been peer reviewed and accepted for publication but have not yet been edited.

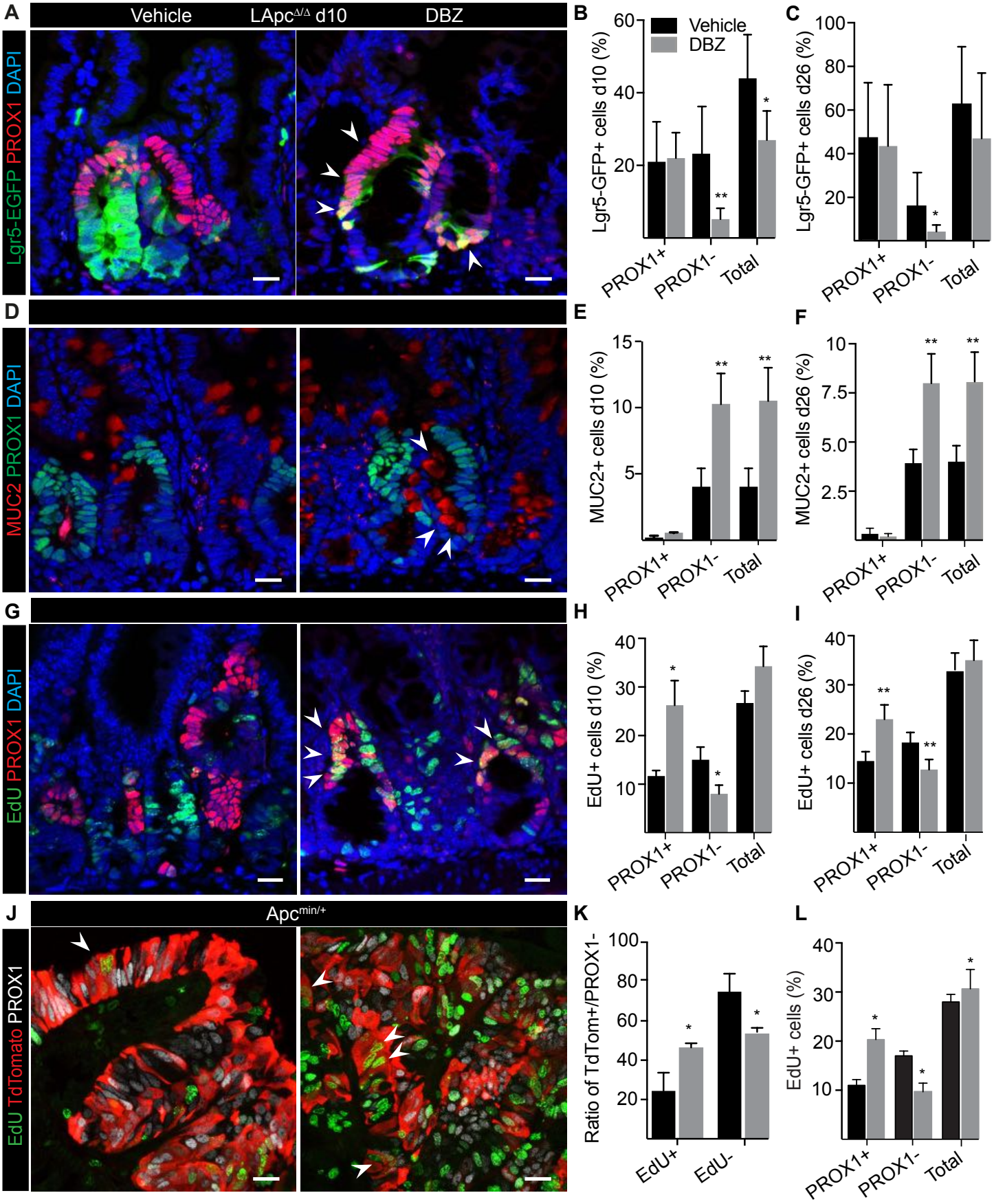

Högström *et al.* Figure 3

Author Manuscript Published OnlineFirst on August 28, 2018; DOI: 10.1158/0008-5472.CAN-18-0451
Author manuscripts have been peer reviewed and accepted for publication but have not yet been edited.

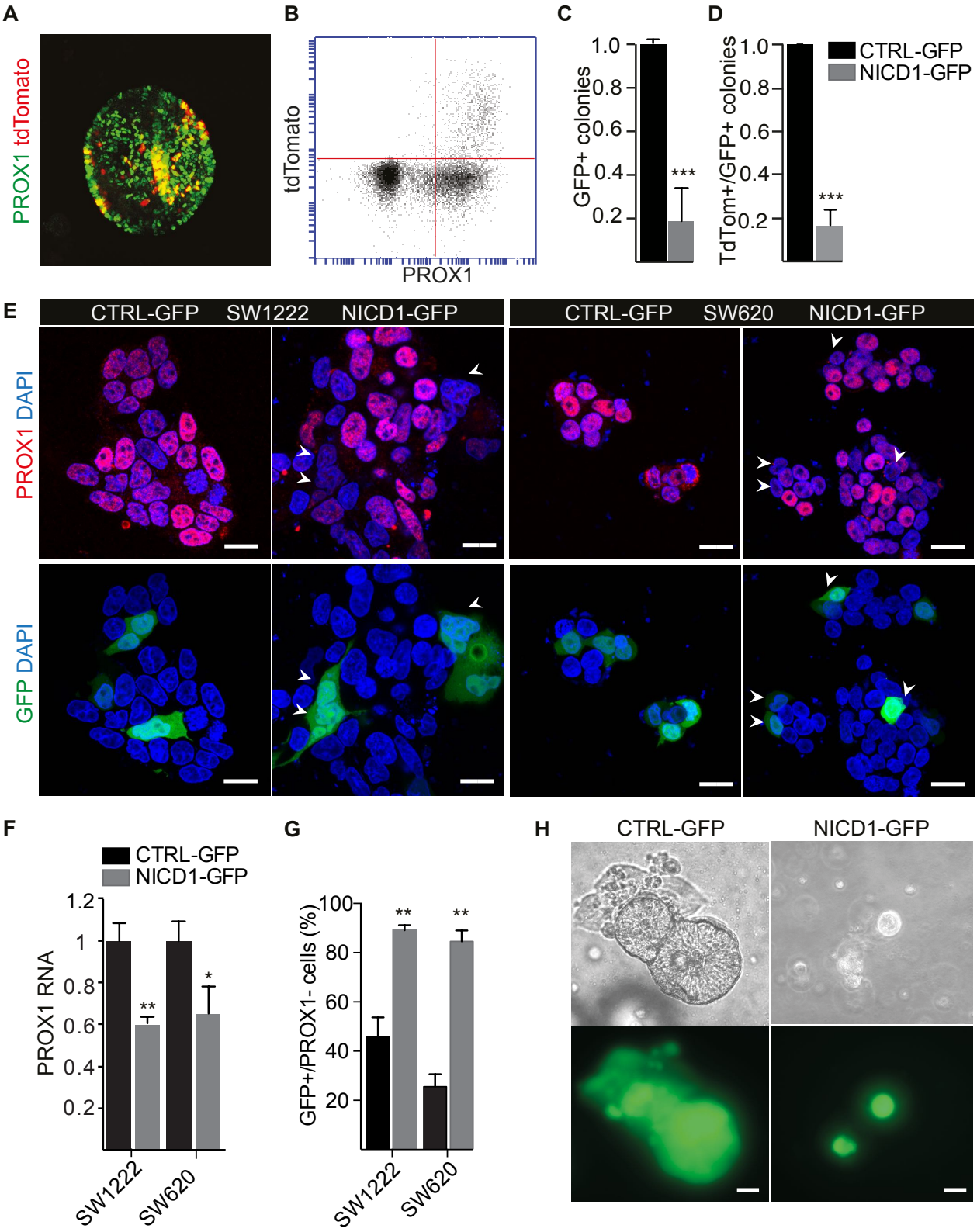

Högström *et al.* Figure 4

Author Manuscript Published OnlineFirst on August 28, 2018; DOI: 10.1158/0008-5472.CAN-18-0451
Author manuscripts have been peer reviewed and accepted for publication but have not yet been edited.

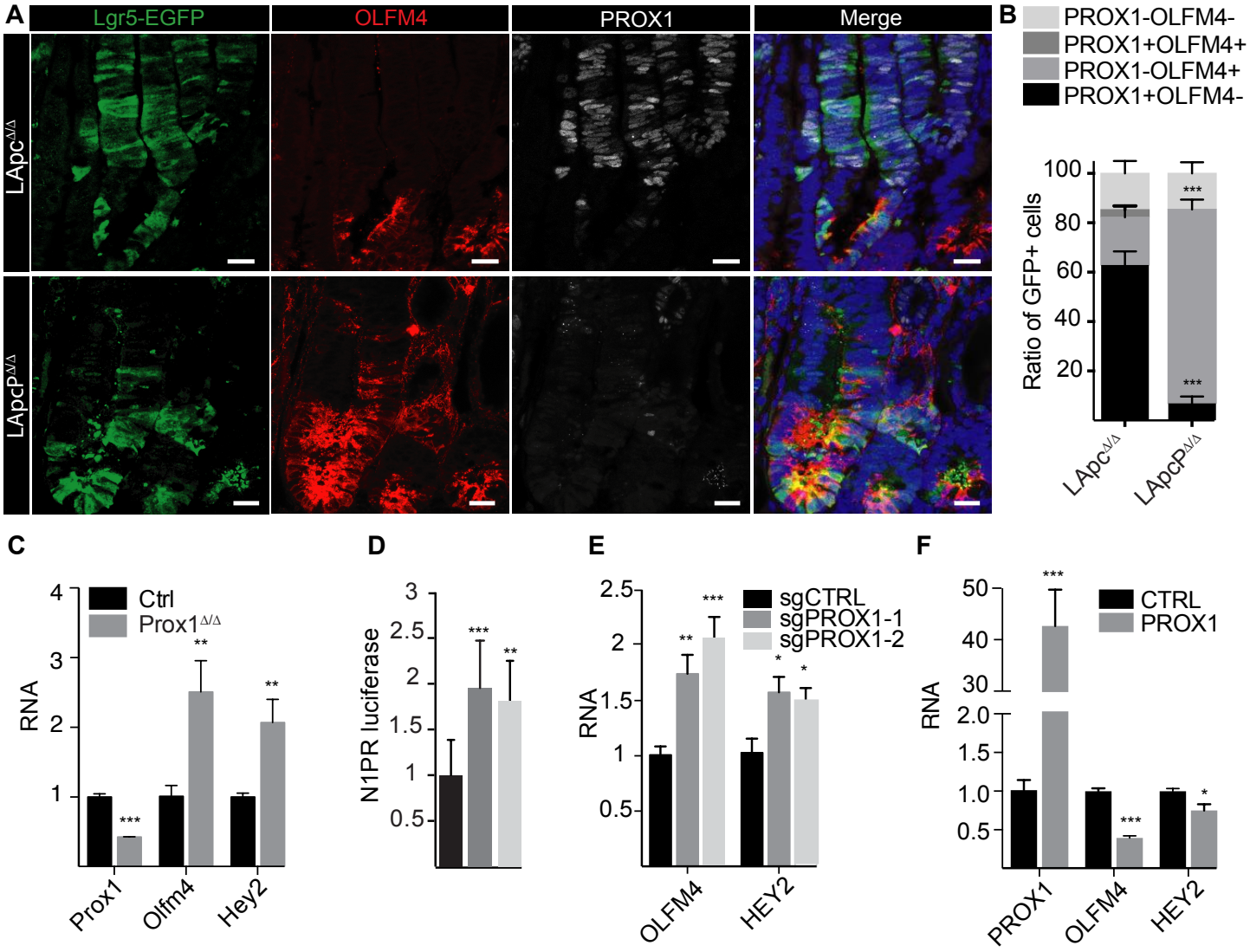

Högström *et al.* Figure 5

Author Manuscript Published OnlineFirst on August 28, 2018; DOI: 10.1158/0008-5472.CAN-18-0451
Author manuscripts have been peer reviewed and accepted for publication but have not yet been edited.

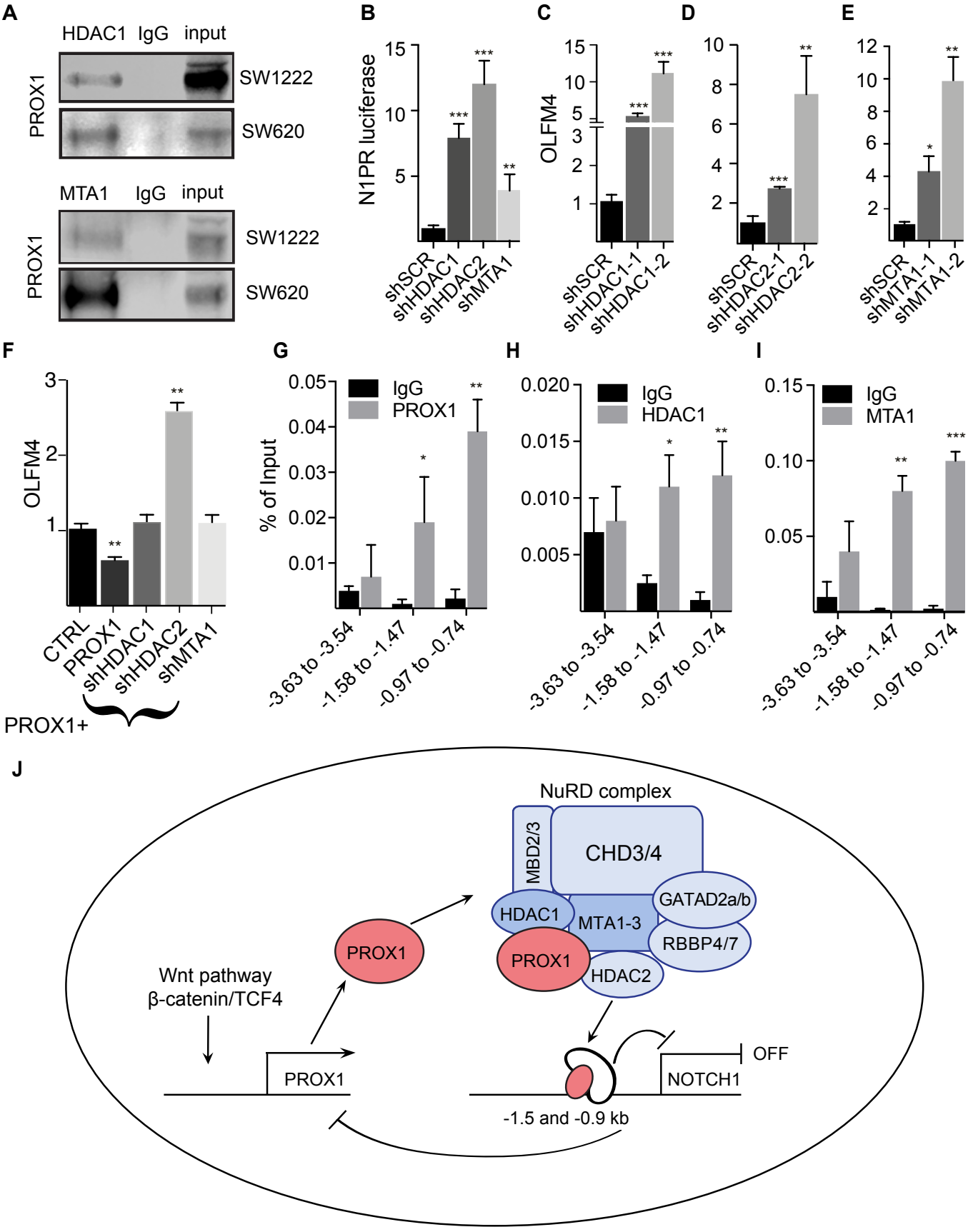

Högström *et al.* Figure 6

AACR American Association for Cancer Research

Cancer Research

The Journal of Cancer Research (1916–1930) | The American Journal of Cancer (1931–1940)

Transcription factor PROX1 suppresses Notch pathway activation via the nucleosome remodeling and deacetylase complex in colorectal cancer stem-like cells

Jenny Högström, Sarika Heino, Pauliina Kallio, et al.

Cancer Res Published OnlineFirst August 28, 2018.